Nonlinear dynamics in wurtzite InN diodes under terahertz radiation*

Feng Wei(冯 伟)†

Department of Physics, Jiangsu University, Zhenjiang 212013, *China*

(Received 9 September 2011; revised manuscript received 3 October 2011)

We carry out a theoretical study of nonlinear dynamics in terahertz-driven n^+nn^+ wurtzite InN diodes by using time-dependent drift diffusion equations. A cooperative nonlinear oscillatory mode appears due to the negative differential mobility effect, which is the unique feature of wurtzite InN aroused by its strong nonparabolicity of the Γ_1 valley. The appearance of different nonlinear oscillatory modes, including periodic and chaotic states, is attributed to the competition between the self-sustained oscillation and the external driving oscillation. The transitions between the periodic and chaotic states are carefully investigated using chaos-detecting methods, such as the bifurcation diagram, the Fourier spectrum and the first return map. The resulting bifurcation diagram displays an interesting and complex transition picture with the driving amplitude as the control parameter.

Keywords: nonlinear dynamics, terahertz radiation, wurtzite InN

PACS: 73.61.Ey, 73.50.Fq, 85.30.Fg, 85.30.De **DOI:** 10.1088/1674-1056/21/3/037306

1. Introduction

During the last few years, InN has attracted considerable attention. It has been studied intensively because of its unusual characteristics such as small effective mass,[1,2] large electron drift velocities,[3,4] surface electron accumulation layer,[5] and the controversy in its bandgap.[6,7] Recent progress in InN epitaxial growth has led to monocrystalline wurtzite InN with improved quality and high mobilities.[8] A band gap around 0.7 eV has been established both experimentally and theoretically.[6,9−11] These unique properties have not only attracted a lot of scientific interest but also opened up many device application possibilities,[12] for example, high-speed high-frequency electronics,[13] electron emitters, detectors,[14] and solar cells.[15] One unique feature of wurtzite InN is that it has the largest peak velocity and negative differential mobility (NDM) region according to the theoretical studies of the steady-state transport characteristics using ensemble Monte Carlo (MC) simulations,[16,17] making this material very attractive for high-frequency applications. The NDM effect in InN is associated with a strong nonparabolicity of the Γ_1 valley rather than with the intervalley transfer, different from what is observed for semiconductors such as GaAs.[18] The NDM region can especially result in some interesting phenomena, such as current self-oscillation and complex nonlinear dynamics in different kinds of semiconductor systems.[19,20]

In this article, we present a study of nonlinear dynamics of the NDM n^+nn^+ InN diode driven by a THz signal and a dc bias. We investigate possible modes of current oscillations with the dc bias, the doping concentration, and the intensity of the radiation as controlling parameters. The transitions between the periodic and chaotic states are examined by different chaos-detecting methods, such as the Poincaré bifurcation diagram, the power spectrum and a first return map. The resulting power spectrum pattern displays a very complex mosaic scenario with a self-similar emergence of high-order mixing frequencies.

2. Negative differential mobility of electrons in wurtzite InN

Recent experiments have been performed on high-quality samples with low free-electron concentration and relevant theoretical studies have revealed that the fundamental gap of wurtzite InN is very small, in a range of 0.7–1.0 eV, depending on the electron concentration.[11,21] A direct consequence of the narrow gap of InN is the strong nonparabolicity of the

*Project supported by Jiangsu University Initial funding for advanced talents, China (Grant No. 11JDG037).

†Corresponding author. E-mail: xfhe@ujs.edu.cn

© 2012 Chinese Physical Society and IOP Publishing Ltd

lowest conduction band. A simple analytical form of the nonparabolic dispersion for the conduction band of InN can be obtained from Kane's Hamiltonian:[22]

$$E_{\rm c}(k) = \frac{\hbar^2 k^2}{2m_0} + \frac{1}{2}\left(E_{\rm g}^{+} + \sqrt{(E_{\rm g}^{-})^2 + 4E_{\rm p}\cdot\frac{\hbar^2 k^2}{2m_0}}\right), \tag{1}$$

where $E_{\rm g}^{\pm} = E_{\rm g} \pm \Delta_1$ and $E_{\rm g} = 0.72$ eV is the intrinsic band gap energy, $\Delta_1 = 0.067$ eV,[23] m_0 is the electron rest mass, and $E_{\rm p} = 2|\langle S|p_z|Z\rangle|^2/m_0$ is an energy parameter related to the $\boldsymbol{k}\cdot\boldsymbol{p}$ matrix element, and is typically ∼10 eV–15 eV.

The conduction band of wurtzite InN by the $\boldsymbol{k}\cdot\boldsymbol{p}$ fit using Eq. (1) exhibits a deviation from the parabolic shape in InN. The reported dependence of the conduction band effective mass on the free carrier concentration in InN indicates a pronounced nonparabolicity of the conduction band,[1,24] and this nonparabolicity in the main conduction band valley alone can lead to a negative differential mobility in semiconductors.[25] InN demonstrates the largest peak velocity among GaN, GaAs, and $In_{0.53}Ga_{0.47}As$, making this material very attractive for high-frequency applications. The NDM effect in InN is associated with a strong nonparabolicity of the Γ_1 valley rather than with the intervalley transfer, which is different from what is observed for semiconductors such as GaAs.[18] The analytical fit for the velocity-field relation is as follows:

$$V_{\rm d}(E) = \frac{4073.57E}{11694.68 + 5.43\times10^{-9}E^{1.94}}, \tag{2}$$

which is shown in Fig. 1 with $V_{\rm d}$ being the drift velocity, and E the electric field. In the whole range of electric field considered here, a good agreement is observed between the analytical results (line) and the EMC calculations (solid squares).[26] Figure 1 gives us a clear picture of NDM of wurtzite InN. We can see that the peak velocity is $v_{\rm d}^{\rm M} = 5.05\times10^5$ m/s when the electric field increases to $F_{\rm T} = 32$ kV/cm. At lower fields than this it is not ohmic, while for higher intensities nonlinear transport follows. Therefore, the current increasing less markedly with E, that is, the differential mobility ${\rm d}V_{\rm d}/{\rm d}E$ keeps decreasing with increasing E. Intensive scattering of the hot electrons with energy beyond the optical phonon scattering threshold can be considered as the reason of this decrease.[27]

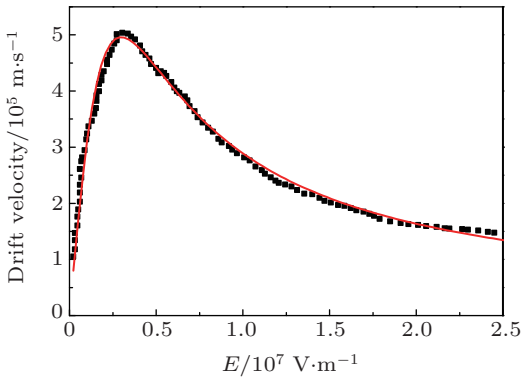


Fig. 1. (colour online) Analytical fit for the velocity-field relation at electron density $N_{\rm d} = 10^{17}$ cm^{-3} and lattice temperature $T = 77$ K.

3. Transitions between periodic and chaotic states in wurtzite InN

Combining the transient drift-diffusion equations,[28,29] we can obtain the total current density. The electrostatic potential $\phi(x,t)$ and electron density $n(x,t)$ are the time- and space-dependent fundamental unknown variables that we need to solve. The total current density is the sum of the conduction current density $j(x,t)$ and the displacement current density and expressed as

$$J(t) = j(x,t) + \kappa\varepsilon_0\frac{\partial E(x,t)}{\partial t}, \tag{3}$$

where $\kappa\varepsilon_0$ is the dielectric constant, the n-base length of the n^+nn^+ InN diode is set to be $l = 0.5$ μm and the lattice temperature is $T = 77$ K. Here, we deal with the InN diode subjected to dc and ac voltages in the form of

$$V(t) = V_{\rm dc} + V_{\rm ac}\sin(2\pi f_{\rm ac}t), \tag{4}$$

where $V_{\rm ac}$ is the driving amplitude and $f_{\rm ac}$ is the driving frequency of the ac voltage. The boundary conditions for $\phi(x,t)$ and $n(x,t)$ are as follows:

$$\phi(x_{\rm L},t) = 0, \quad \phi(x_{\rm R},t) = V(t), \tag{5}$$

$$n(x_{\rm L},t) = N_{\rm d}(x_{\rm L}), \quad n(x_{\rm R},t) = N_{\rm d}(x_{\rm R}). \tag{6}$$

When the external ac voltage is applied to the dc voltage biased self-oscillating InN system, a typical nonlinear system is constructed and the oscillation frequency of the InN system strongly depends on the amplitude of the ac voltage bias. Therefore, we choose the ac amplitude $v_{\rm ac}$ as the control parameter to

investigate the nonlinear dynamics of the InN system. In the simulations, 300 space meshpoints are chosen and the time step is set to be $1/f_{\rm ac}/2000$. The ac frequency is fixed to be the inverse golden mean G [$\equiv (1+\sqrt{5})/2 = 1.618\cdots$] times the self-oscillating frequency $f_{\rm s}$, i.e., $f_{\rm ac} = G \times f_{\rm s}$. The inverse golden mean ratio is often used in driving nonlinear systems,[20,30–32] because under this condition the driving frequency is incommensurate and the richest nonlinear structure of different mode mixings may appear. Here, we investigate the nonlinear dynamics of an InN diode at $V_{\rm dc} = 1.8$ V, $N_{\rm d} = 1 \times 10^{17}$ cm^{-3} and $V_{\rm dc} = 2$ V, $N_{\rm d} = 2 \times 10^{17}$ cm^{-3}, respectively. A variety of spatiotemporal behaviours have been found when the n^+nn^+ InN diode is subjected to a periodic voltage expressed by Eq. (2), depending on the dc bias $V_{\rm dc}$ and ac amplitude $V_{\rm ac}$.

First, we carry out some simulations with the dc voltage fixed to be $V_{\rm dc} = 1.8$ V and the doping concentration $N_{\rm d} = 1.0\times10^{17}$ cm^{-3} at $T = 77$ K. In this case, the self-oscillating frequency $f_{\rm s}$ is 1.43 THz. To clarify the periodic and chaotic regions in controlling the parameter space of $V_{\rm ac}$, we calculate the Poincaré bifurcation diagram and power spectrum diagram with $V_{\rm ac}$ changing from 0 to 0.45 V. Let $T_{\rm ac} = 1/f_{\rm ac}$ be the period of the ac driving signal. For each value of ac amplitude $V_{\rm ac}$, we adopt the current density at times $t_m = mT_{\rm ac}$ ($m = 1, 2, 3, \ldots$) as our Poincaré mapping. The Poincaré bifurcation diagram for the chaotic solution contains a large number of points, while the periodic one contains only several points. Therefore, the chaotic regions can be easily distinguished from the periodic ones. Figures 2(a) and 2(b), respectively, show the Poincaré bifurcation diagram and power spectrum diagram at $V_{\rm dc} = 1.8$ V, $N_{\rm d} = 1.0 \times 10^{17}$ cm^{-3} and $f_{\rm ac} \approx 1.43$ THz. When $V_{\rm ac} < 0.122$ V, the solution of the system is chaotic, distinguished by having a number of points in the bifurcation diagram for each $V_{\rm ac}$. As $V_{\rm ac}$ approaches 0.122 V, the chaotic behaviour disappears abruptly and a 5-periodic window appears with the frequency spectra consisting of $m/5$ ($m = 1, 2, 3, \ldots$) times the driving frequency $f_{\rm ac}$. When $V_{\rm ac}$ approaches 0.253 V, the solutions become seven-periodic and when $V_{\rm ac} >$ 0.418 V, the solutions are attracted to one periodic orbit. With $V_{\rm ac}$ increasing, 5-, 7- and 1-periodic windows are observed, and the widths of the windows become narrower and narrower as the frequency of the solution increases. Outside these periodic windows, the solutions are chaotic. Figure 2(b) shows the power spectra as a density plot, which is obtained by Fourier transformation of the time-dependent current density $J(t)$. In the Fourier spectrum bifurcation diagram, light areas correspond to larger amplitudes of the Fourier spectrum than the dark areas. The transitions between periodic and chaotic states can be easily observed from Fig. 2(b). In the chaotic regions, the Fourier spectra are very irregular with many peaks corresponding to the light area, while for the n-periodic regions, the Fourier spectra display peaks at i/n ($i = 1, 2, 3, \ldots$) times the driving frequency $f_{\rm ac}$. Near the left and right axes of Fig. 2(b), we show the positions of self-oscillating fundamental frequencies $nf_{\rm s}$, that is n/G ($n = 1, 2, 3$), and the driving frequencies $mf_{\rm ac}$ ($m = 1, 2$). The power spectrum diagram clearly indicates the coupling of dc bias and ac driving voltage and that with the ac voltage increasing, the $f_{\rm ac}$ line becomes lighter and thinner while the $f_{\rm s}$ line becomes darker and thicker and finally disappears, which indicates that the ac voltage plays an increasing role in the behaviour of carrier motion.

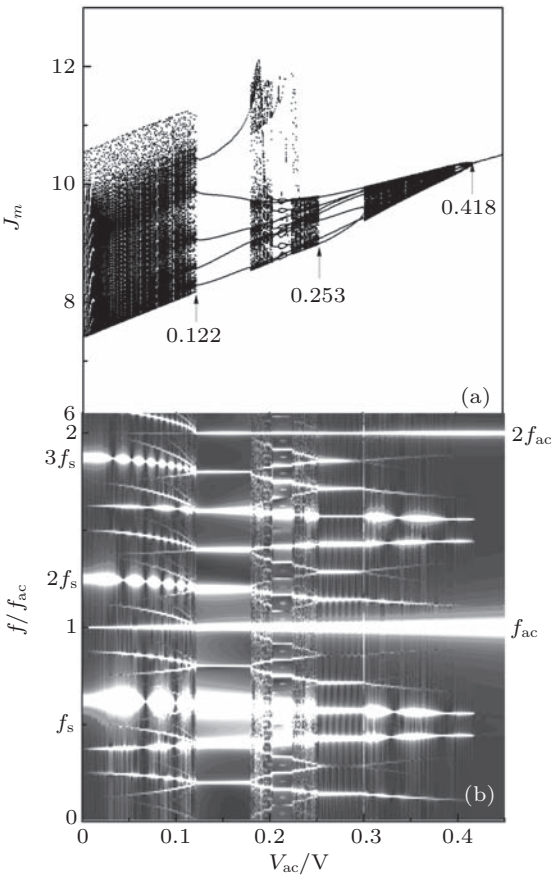


Fig. 2. (a) Poincaré bifurcation diagram and (b) power spectrum bifurcation diagram at $T = 77$ K, $N_{\rm d} = 1 \times 10^{17}$ cm^{-3}, $V_{\rm dc} = 1.8$ V, $f_s = 1.43$ THz, and $f_{\rm ac} = G \times f_{\rm s} \approx 2.313$ THz with G being the inverse Golden mean ratio.

In Fig. 3 the first return maps for four specific ac voltages are given. It provides us with further help to distinguish the chaotic state from the periodic one in the way that the attractors for m-periodic solutions are just the m separate points while those for the chaotic solutions are infinite random points (when $m \to \infty$).

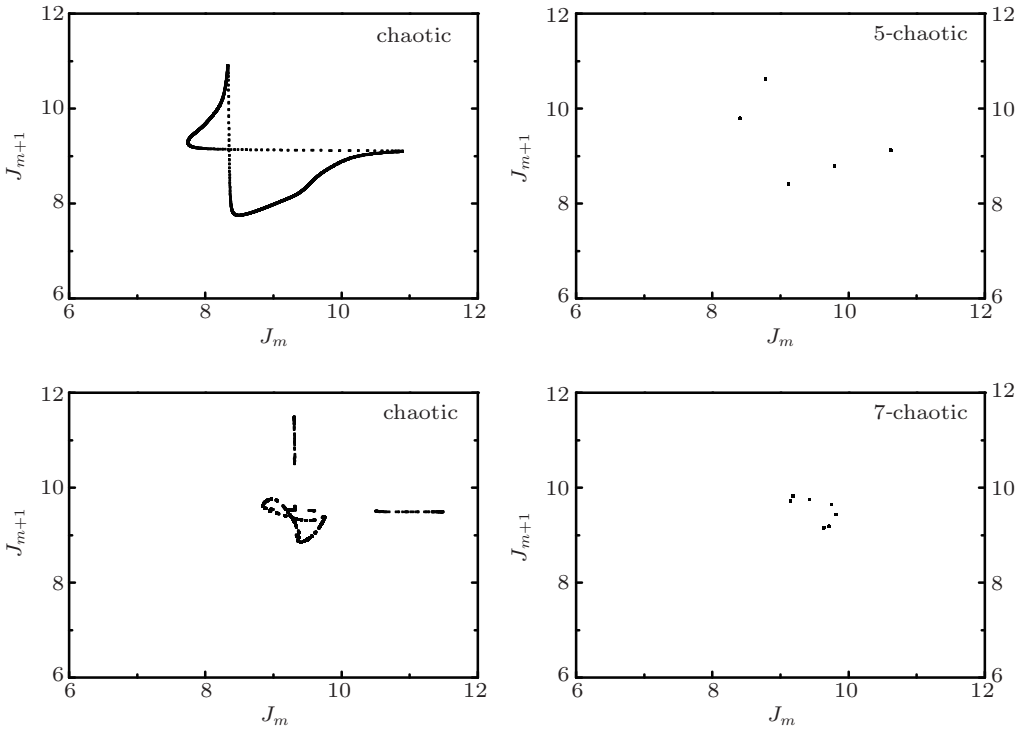


Fig. 3. First return maps at (a) $V_{\rm ac} = 0.055$ V, (b) 0.15 V, (c) 0.23 V, and (d) 0.27 V, respectively, for the NDM n^+nn^+ diode described in Fig. 2.

We also study the self-oscillating InN system biased at $V_{\rm dc} = 2$ V, $N_{\rm d} = 2 \times 10^{17}$ cm^{-3}. This dc voltage leads to a natural oscillation frequency at $f_{\rm s} = 0.91$ THz and the driving frequency is fixed at $f_{\rm ac} = G \times f_{\rm s} = 1.47$ THz. More complicated Poincaré and Fourier spectrum bifurcation diagrams are shown in Fig. 4. From the Poincaré bifurcation diagram we can see that the oscillation changes its behaviour between the periodic and chaotic states, that with $V_{\rm ac}$ increasing the periodic window becomes narrower and narrower and the number of the periodic solutions becomes smaller and smaller. When $V_{\rm ac} > 0.882$ V, the temporal solutions of the nonlinear InN system become synchronous with the driving signal. Figure 4(b) depicts the Fourier spectrum bifurcation diagram of InN system. As mentioned in the above paragraph, the peaks of the n-periodic windows appear at frequencies $f = (i/n)f_{\rm ac}$. The 7-periodic solutions are clearly observed in the region of $0.171 < f_{\rm ac} < 0.198$ V. While in the region of $0.376 < f_{\rm ac} < 0.556$ V, the 2-periodic solutions can also be clearly observed. For the ac amplitude above 0.882 V, the peaks of the solution occur at $f = if_{\rm ac}$, which indicates the synchronization between the nonlinear oscillation and the external driving oscillation.

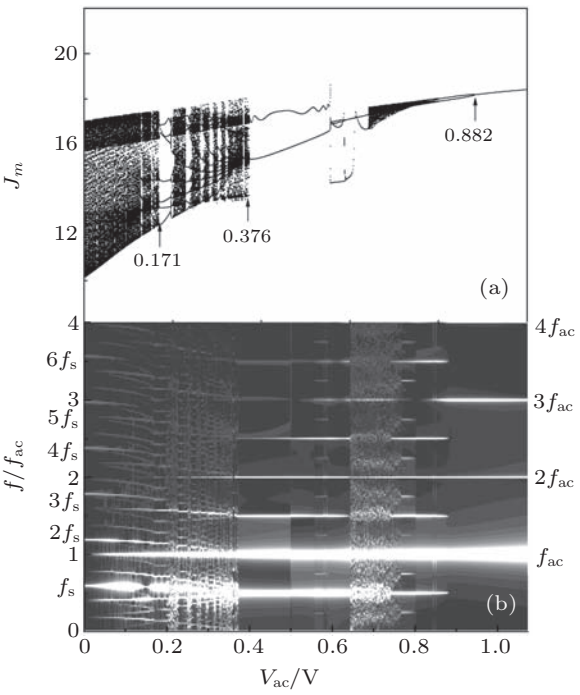


Fig. 4. (a) Poincaré bifurcation diagram and (b) power spectrum bifurcation diagram at $T = 77$ K, $N_{\rm d} = 2 \times 10^{17}$ cm^{-3}, $V_{\rm dc} = 2$ V, $f_s = 0.91$ THz, and $f_{\rm ac} = G \times f_{\rm s} \approx 1.47$ THz.

4. Conclusion

According to the transient drift-diffusion model, we theoretically investigate nonlinear dynamical characteristics of n^+nn^+ wurtzite InN diodes subjected to dc bias and THz electromagnetic radiation. The NDM effect in wurtzite InN associated with a strong nonparabolicity of the Γ_1 valley has been reported in the literature. The InN diodes can produce a cooperative nonlinear oscillatory mode which leads to a complicated chaotic dynamics. The Poincaré bifurcation diagram, power spectrum, and the first return map are calculated to clarify the transition between the periodic and the chaotic states. By changing the dc bias, the doping concentration and ac amplitude, various types of spatiotemporal behaviours and current-voltage characteristics have been found. The resulting power spectrum pattern displays a very complex mosaic scenario with a self-similar emergence of high-order mixing frequencies. The present study may be useful for utilizing and controlling the possible chaos in opto-electronic devices with wurtzite InN.

References

[1] Wu J, Walukiewicz W, Shan W, Yu K M, Ager J W, Haller E E, Lu H and Schaff W J 2002 *Phys. Rev.* B **66** 201403

[2] Nag B R 2003 *Phys. Status Solidi* B **237** R1

[3] Foutz B E, O'Leary S K, Shur M S and Eastman L F 1999 *J. Appl. Phys.* **85** 7727

[4] Tsen K T, Poweleit C, Ferry D K, Lu H and Schaff W J 2005 *Appl. Phys. Lett.* **86** 222103

[5] Mahboob I, Veal T D, McConville C F, Lu H and Schaff W J 2004 *Phys. Rev. Lett.* **92** 036804

[6] Davydov V Y, Klochikhin A A, Seisyan R P, Emtsev V V, Ivanov S V, Bechstedt F, Furthmuller J, Harima H, Mudryi V, Aderhold J, Semchinova O and Graul J 2002 *Phys. Status Solidi* B **229** R1

[7] Nanishi Y, Saito Y and Yamaguchi T 2003 *Jpn. J. Appl. Phys.* Part 1 **42** 2549

[8] Swartz C H, Tomkins R P, Myers T H, Lu H and Schaff W J 2005 *Phys. Status Solidi* C **2** 2250

[9] Rinke P, Winkelnkemper M, Qteish A, Bimberg D, Neugebauer J and Scheffler M 2008 *Phys. Rev.* B **77** 075202

[10] Fuchs F, Furthmüller J, Bechstedt F, Shishkin M and Kresse G 2007 *Phys. Rev.* B **76** 115109

[11] Polyakov V M, Schwierz F, Fuchs F, Furthmüller J and Bechstedt F 2009 *Appl. Phys. Lett.* **94** 022102

[12] Bhuiyan A G, Hashimoto A and Yamamoto A 2003 *J. Appl. Phys.* **94** 2779

[13] O'Leary S K, Foutz B E, Shur M S and Eastman L F 2006 *Appl. Phys. Lett.* **88** 152113

[14] Lu H, Schaff W J and Eastman L F 2004 *J. Appl. Phys.* **96** 3577

[15] Yamamoto A, Tsujino M, Ohkubo M and Hashimoto A 1994 *Sol. Energy Mater. Sol. Cells* **35** 53

[16] Bellotti E, Doshi B K, Blennan K F, Albrecht J D and Ruden P P 1999 *J. Appl. Phys.* **85** 916

[17] Veal T D, McConville C F and Schaff W J 2009 *Indium Nitride and Related Alloys* (Florida: CRC Press)

[18] Fitzer N, Kuligk A, Redmer R, Städele M, Goodnick S M and Schattke W 2003 *Phys. Rev.* B **67** 201201

[19] Cao J C 2003 *Phys. Rev. Lett.* **91** 237401

[20] Feng W and Cao J C 2009 *J. Appl. Phys.* **106** 033708

[21] Wu J Q 2009 *J. Appl. Phys.* **106** 011101

[22] Rinkea P, Scheffler M, Qteish A, Winkelnkemperb M, Bimberg D and Neugebauer J 2006 *Appl. Phys. Lett.* **89** 161919

[23] Stampfl C and Van de Walle C G 1999 *Phys. Rev.* B **59** 5521

[24] Walukiewicz W, Li S X, Wu J, Yu K M, Ager III J W, Haller E E, Lu H and Schaff W 2004 *J. Cryst. Growth* **269** 119

[25] Hauser J R, Glisson T H and Littlejohn M A 1979 *Solid-State Electronics* **22** 487

[26] Polyakov V M and Schwierz F 2006 *Appl. Phys. Lett.* **88** 032101

[27] Masyukov N A and Dmitriev A V 2011 *J. Appl. Phys.* **109** 023706

[28] Cao J C, Liu H C and Lei X L 2000 *J. Appl. Phys.* **87** 2867

[29] Feng W and Cao J C 2008 *J. Appl. Phys.* **104** 013111

[30] Zhang Y H, Kastrup J, Klann R, Ploog K H and Grahn H T 1996 *Phys. Rev. Lett.* **77** 3001

[31] Cao J C, Liu H C, Lei X L and Perera A G U 2001 *Phys. Rev.* B **63** 115308

[32] Wang C and Cao J C 2009 *Chaos* **19** 033136